Nordic Optical Telescope Scientific Association

Active Optics

on the

Nordic Optical Telescope

Mirror Control Algorithms

Mette Owner Petersen
Ole Brix Larsen

December 1991

Active Optics

on the

Nordic Optical Telescope

Mirror Control Algorithms

Mette Owner Petersen
Ole Brix Larsen

December 1991

Contents

1) Introduction

This report presents a description of the mirror controls to be performed in connection with the installation of active optics in 1992 on NOT at La Palma. At the present NOT is equipped with a wavefront sensor providing the lowest order Zernike coefficients of the aberrated wavefront[1], and this report gives a quantitative evaluation of the translations of the secondary mirror (M2) and the deformations of the primary mirror (M1) necessary to control these aberrations. The estimates of the M1 deformations are based upon an expansion of the Zernike polynomials in the lowest order modal shapes of M1[2] (minimum energy modes). This ensures a smooth pattern of the actuator forces and the corresponding deformations, but the aberrated wavefront will not be corrected perfectly. The degree of correction which can be obtained is estimated as the ratio of the wavefront aberration variance (WAV) after correction to the WAV before correction for the individual Zernike aberration terms. The modal shapes, the corresponding point force patterns and the resulting M1 deformation patterns are derived by FE (finite element) calculations on M1. The correct linear combinations of the excited deformation patterns to produce (or compensate) given Zernike aberrations are determined by least squares fits.

2) Aberration description and wavefront sensing

The wavefront aberrations $W(\rho,\varphi)$ corresponding to the axial image point, where ρ is the normalized radius vector and φ is the polar angle in the pupil, can be described as an expansion in quasi Zernike polynomials[2]:

$$W(\rho,\varphi) = \sum_q a_q Z_q(\rho,\varphi,\theta_q) \qquad (1)$$

where

$$Z_q = \rho^m \cos(n\varphi + \theta_q) \qquad (2)$$

m even: n = 0, 2, 4,.....m
m uneven: n = 1, 3, 5, ...m

To fourth order in ρ, these polynomials are listed below:

$Z_0 = 1$	Const. phaseshift
$Z_1 = \rho\cos(\varphi + \theta_1)$	Tilt
$Z_2 = \rho^2$	Defocus
$Z_3 = \rho^3\cos(\varphi + \theta_3)$	Decentering coma
$Z_4 = \rho^4$	Spherical aberration
$Z_5 = \rho^2\cos(2\varphi + \theta_5)$	Astigmatism
$Z_6 = \rho^3\cos(3\varphi + \theta_6)$	Triangular coma
$Z_7 = \rho^4\cos(2\varphi + \theta_7)$	Fifth order astigmatism
$Z_8 = \rho^4\cos(4\varphi + \theta_8)$	Quadratic astigmatism

The first three polynomials are related to zero point choices, whereas the remaining polynomials represent wavefront distortions deteriorating the ultimate image quality. Note that discarding Z_7 from the list, the remaining five distortion polynomials will be mutually orthogonal due to the φ dependance. For this reason we do not attempt to correct fifth order astigmatism.
At NOT the total wavefront aberration is measured by the Korhonen - Hartmann interferometric wavefront sensor[1]. By means of auxiliary software the output of the sensor is the five coefficients:

a_3, a_4, a_5, a_6, and a_8

and the five angles (related to an arbitrary zero position):

θ_3, θ_5, θ_6 and θ_8

It is the intention to correct decentering coma by transverse M2 translation and the remaining aberrations by M1 deformations.
Also provided by the wavefront sensor are the tilt parameters a_1 and θ_1 and the defocus parameter a_2. Hence there will be a possibility to estimate both tilt and defocus relative to fixed zeros defined by the wavefront sensor.

3) Aberration control by M2 translations

In order to estimate the effects of the M2 translations, the general layout of NOT shown in Fig. 1 has to be considered.

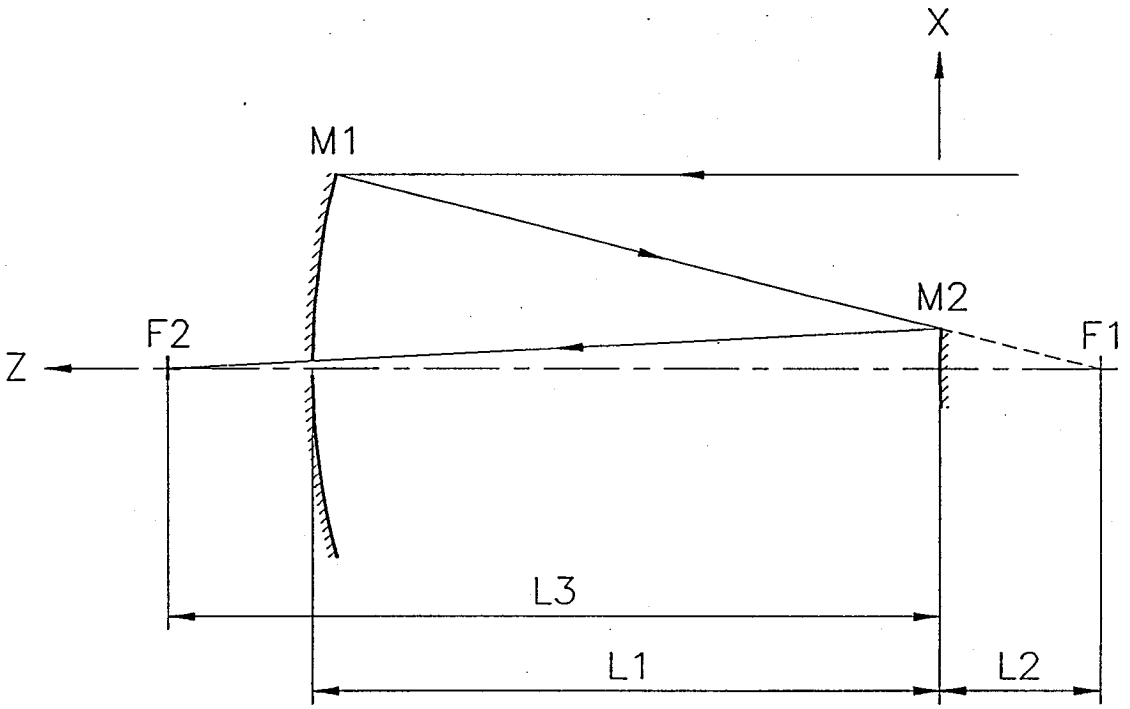

Fig. 1

NOT is a Ritchey Chrétien telescope with two hyperbolic mirrors providing a design free of spherical aberration and coma. The incoming starlight is focussed virtually by M1 in F1 and brought to a final focus in F2 by reflection in M2. Relevant distances, apertures and mirror curvatures taken from [4] are listed below:

L_1		= 4184.308 mm	
L_2		= 935.692 mm	
L_3		= 5146.297 mm	
f	$= L_3(L_1 + L_2)/L_2$	= 28160 mm	Focal length
R_1	$= 2(L_1 + L_2)$	= 10240 mm	M1 radius of curvature
R_2	$= -2L_2L_3/(L_3 - L_2)$	= -2287.248 mm	M2 radius of curvature
b_2		= -2.234127	Aspheric parameter of M2
D_1		= 2560 mm	M1 diameter
F	$= f/D_1$	= 11	Exit focal ratio
D_2	$= L_3/F$	= 467.85 mm	On axis illum. M2 diameter

Denoting by U^- the incident wavefront upon M2 and by U^+ the reflected wavefront, we have:

$$U^+(x,y) = T(x,y)\ U^-(x,y) = \exp(ikW)\ U_0(x,y) \tag{3a}$$

$$T(x,y) = \exp[-2ikz_2(x,y)] \tag{3b}$$

where U_0 is a perfect wavefront converging towards F2 and $z_2(x,y)$ is the position of the M2 surface measured relative to the normal plane through the vertex.
In the case of perfect mirror alignment and separation, we have:

$$U^-(x,y) = \exp[-ik(\frac{x^2+y^2}{2L_2} - W_{SA}(x,y))] \tag{4a}$$

$$U_0(x,y) = \exp[-ik\frac{x^2+y^2}{2L_3}] \tag{4b}$$

$$z_2(x,y) = \frac{x^2+y^2}{2R_2} + \tfrac{1}{2}W_{SA}(x,y) \tag{4c}$$

$$W_{SA}(x,y) = \frac{1+b_2}{4R_2^3}(x^2+y^2)^2 \tag{4d}$$

where W_{SA} is the spherical aberration associated with M2. Insertion of Eqs. (4) in Eqs. (3) yields:

$$U^+(x,y) = \exp[-ik\frac{x^2+y^2}{2L_3}] \tag{5}$$

i.e. W = 0.

Defocus

To lowest order a longitudinal translation δ_l of M2 towards M1 results in $L_2 \rightarrow L_2 + \delta_l$ in Eq. (4a) and $L_3 \rightarrow L_3 - \delta_l$ in Eq. (4b). Use of Eqs. (4) in Eqs. (3) gives to lowest order in δ_l the aberration W related to defocussing

$$W = a_2 \rho^2 \tag{6a}$$

$$\rho^2 = (\frac{2}{D_2})^2 (x^2+y^2) \tag{6b}$$

$$a_2 = \frac{\delta_l}{8(F)^2} [1+(\frac{L_3}{L_2})^2] = 3.23 \times 10^{-2} \delta_l \tag{6c}$$

Hence a longitudinal translation of 31 x 10^{-3} mm of M2 produces an aberration coefficient a_2 of 10^{-3} mm.

Decentering tilt and coma

A transversal displacement δ_t of M2 in the direction of the x axis (see Fig. 1) results in

$$z_2(x,y) = \frac{(x-\delta_l)^2+y^2}{2R_2} + \frac{1+b_2}{8R_2^3} [(x-\delta_l)^2+y^2]^2 \tag{7}$$

which used together with Eqs. (4a,b) in Eqs. (3) gives the decentering aberration W to lowest order in δ_t:

$$W = a_1\ \rho\ \cos(\varphi) + a_3\ \rho^3\ \cos(\varphi) \tag{8a}$$

$$\rho\ \cos(\varphi) = \frac{2x}{D_2} \tag{8b}$$

$$a_1 = -\left[1-\frac{L_3}{L_2}\right]\frac{\delta_t}{2F} = -\ 2.04\ x\ 10^{-1}\ \delta_t \qquad (\textit{Tilt}) \tag{8c}$$

$$a_3 = -\ (1+b_2)\left[1-\frac{L_3}{L_2}\right]^3\frac{\delta_l}{64F^3} = -\ 1.32\ x\ 10^{-3}\ \delta_t \qquad (\textit{Decentering coma}) \tag{8d}$$

Hence decentering coma is induced through the spherical aberration term, and will always result in an additional tilt (image translation).
The angular displacement α in the image plane associated with a_1 is given by

$$\alpha = \frac{2Fa_1}{f} = 0.161\ \textit{arcsecs}/\mu m\ a_1 \tag{9}$$
$$\alpha = 24.9\ \textit{arcsecs}/\mu m\ a_3$$

where Eqs. (8c,d) have been used to obtain the last relation.
It is seen that a transversal displacement of 759 x 10^{-3} mm results in a coma coefficient $a_3 = 10^{-3}$ mm and is associated with an angular pointing change of 25 arcsecs.

4) Modal deformations of M1

As mentioned previously, the intention is to control the remaining aberrations by means of the lowest order modal deformations of M1. To this end the modal shapes were estimated by means of FE calculations. Since the actuator support consists of only three rings, it was decided to use only the six lowest order (excitable) modes in order to ensure a not too pathological and noise sensitive force pattern of the actuators. From the modal shapes, the corresponding force patterns in the 45 actuator points leading (as close as possible) to the modal deformations were derived, and the deflections caused by these force patterns were calculated in 720 points in a cylindrical coordinate frame. To ensure static equilibrium, the deflection patterns came out relative to three fix points, and in order to match the Zernike polynomials, tilt and translation had to be subtracted from some of the patterns ensuring orthogonality with respect to the φ dependance. Neglecting a slightly uneven spacing in ρ of the points, this was done minimizing

$$\varepsilon^2 = \Sigma_{\text{all points}}\, \rho(\text{Msn} - b\rho\cos(\varphi) - c)^2$$

with respect to b and c for the modes Msn in question. From this procedure, the coefficients b and c determining the tilt surface to be subtracted from the mode should be calculated from

$$b = \frac{\sum_{all\ points} \rho^2\ Msn(\rho,\varphi)\ \cos(\varphi)}{\sum_{all\ points} \rho^3\ \cos^2(\varphi)} \qquad \textbf{(10a)}$$

$$c = \frac{\sum_{all\ points} \rho\ Msn(\rho,\varphi)}{\sum_{all\ points} \rho} \qquad \textbf{(10b)}$$

Figs. 2 to 7 show the deflection patterns to be used for M1 control. In order to clarify the symmetry properties, a projection of the contour curves is shown at the "bottom" of some of the plots. Note that the patterns can be classified in four mutually orthogonal groups:

Group I (axisymmetric): Ms2 and Ms7 (Figs. 3 and 7) to be used for control of Z_4 (spherical aberration).

Group II (cos(2φ)): Ms1 and Ms6 (Figs. 2 and 6) to be used for control of Z_5 (astigmatism).

Group III (cos(3φ): Ms3 (Fig. 4) to be used for control of Z_6 (triangular coma).

Group IV (cos(4φ): Ms5 (Fig. 5) to be used for control of Z_8 (quadratic astigmatism).

The missing modepattern Ms4 showing cos(φ) dependance, could not be excited, but as shown in the previous section the corresponding aberration (coma) is controlled by M2 translation.

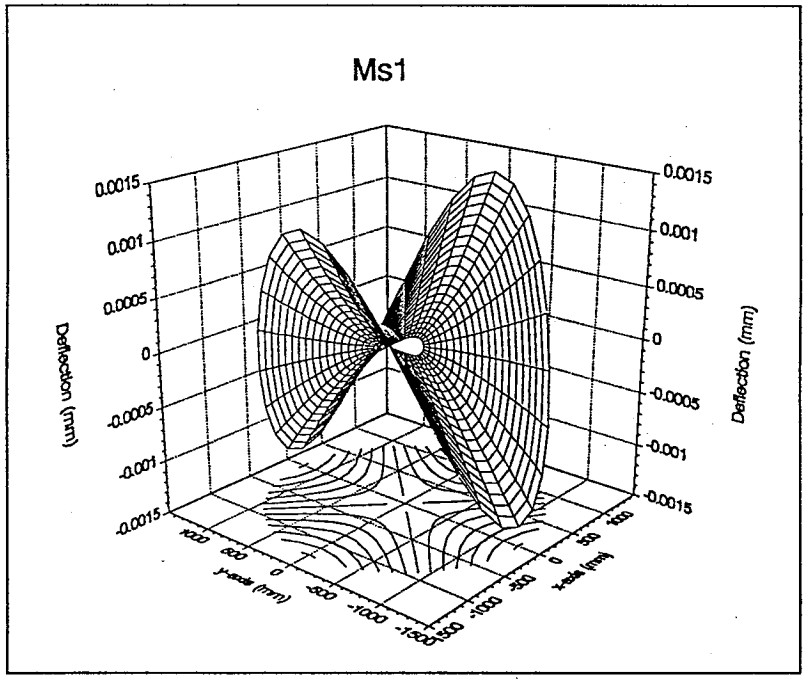

Fig. 2

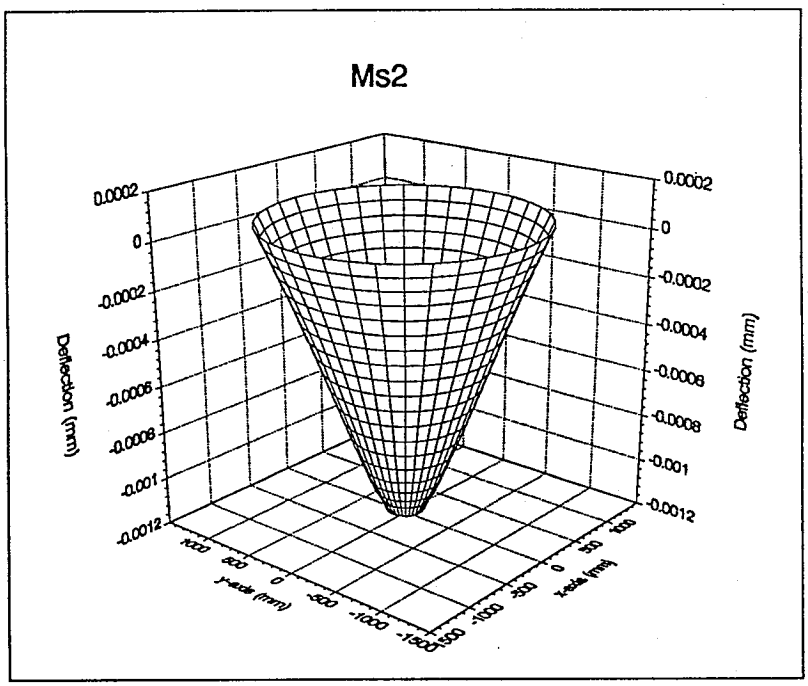
Ms2
Deflection (mm)
0.0002
0
-0.0002
-0.0004
-0.0006
-0.0008
-0.001
-0.0012
y-axis (mm)
1000
500
0
-500
-1000
-1500
x-axis (mm)
-1000
-500
0
500
1000
Deflection (mm)
0.0002
0
-0.0002
-0.0004
-0.0006
-0.0008
-0.001
-0.0012

Fig. 3

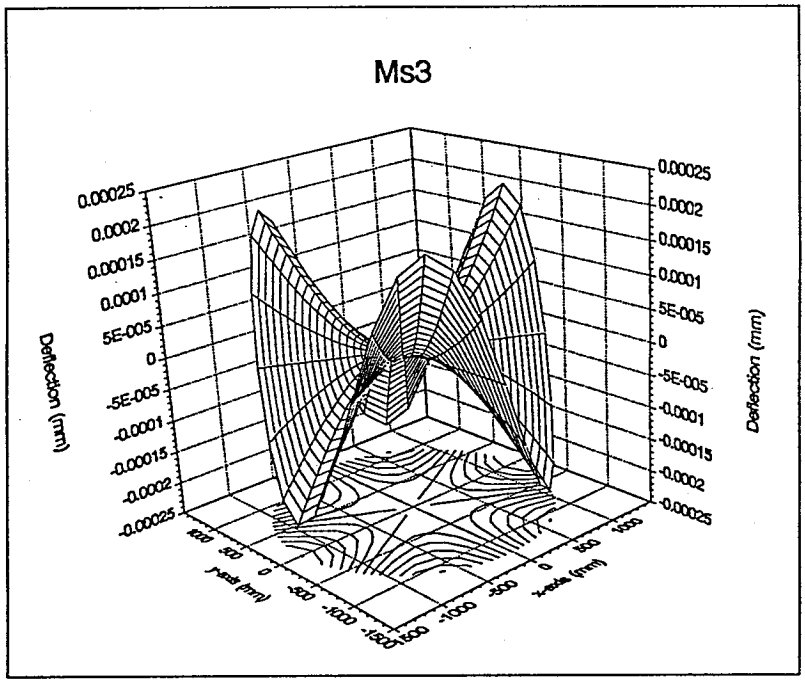
Ms3
Deflection (mm)
0.00025
0.0002
0.00015
0.0001
5E-005
0
-5E-005
-0.0001
-0.00015
-0.0002
-0.00025
y-axis (mm)
1000
500
0
-500
-1000
-1500
x-axis (mm)
-1000
-500
0
500
1000
Deflection (mm)
0.00025
0.0002
0.00015
0.0001
5E-005
0
-5E-005
-0.0001
-0.00015
-0.0002
-0.00025

Fig. 4

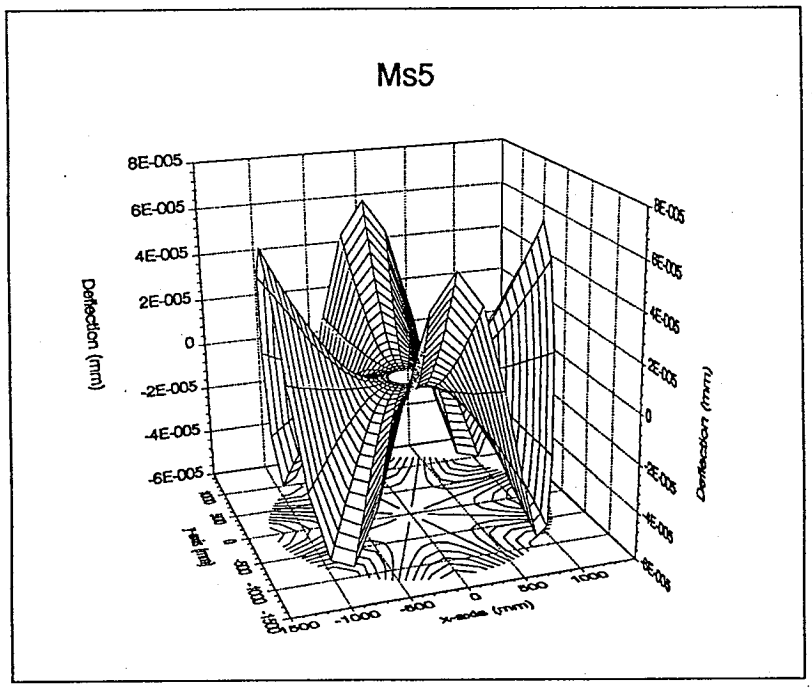
Ms5
8E-005
6E-005
4E-005
2E-005
0
-2E-005
-4E-005
-6E-005
Deflection (mm)
-1500
-1000
-500
0
500
1000
x-axis (mm)
Deflection (mm)

Fig. 5

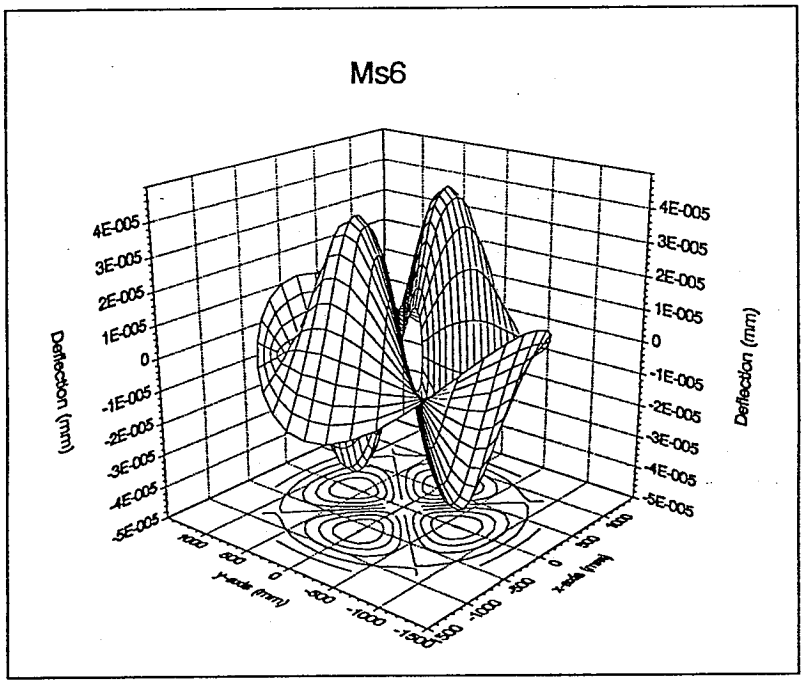
Ms6
4E-005
3E-005
2E-005
1E-005
0
-1E-005
-2E-005
-3E-005
-4E-005
-5E-005
Deflection (mm)
y-axis (mm)
x-axis (mm)
Deflection (mm)

Fig. 6

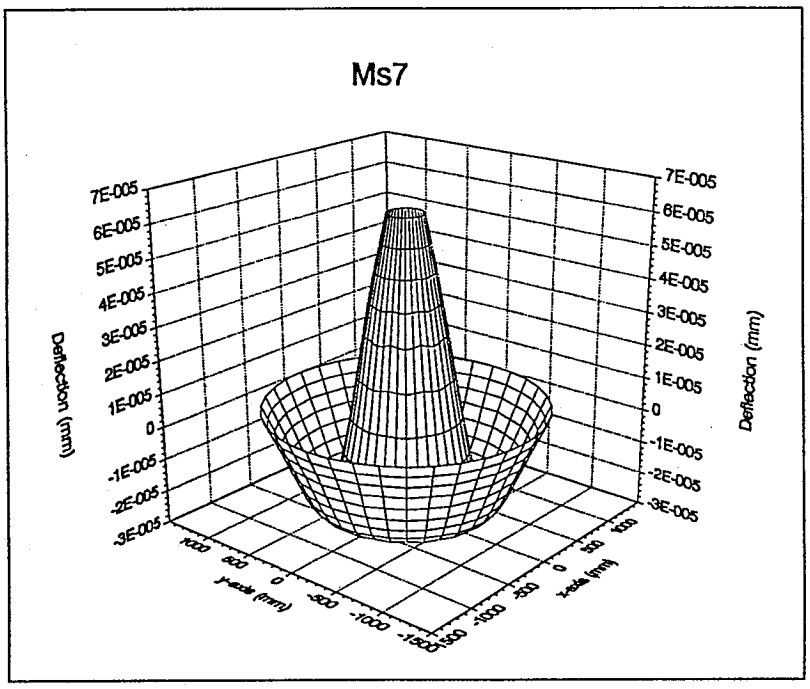
Ms7
7E-005
6E-005
5E-005
4E-005
3E-005
2E-005
1E-005
0
-1E-005
-2E-005
-3E-005
Deflection (mm)
1000
500
0
-500
-1000
-1500
y-axis (mm)
-500
-250
0
250
500
x-axis (mm)

Fig. 7

5) Aberration control by M1 deformations

Given a wavefront aberration pattern described by the expansion Eq. (1) in Zernike polynomials, the part of the wavefront to be corrected here is given as

$$W_z(\rho,\varphi) = \sum_{relevant\ q} a_q Z_q(\rho,\varphi,\theta_q) \qquad \textbf{(11a)}$$

$$Z_q = \rho^m \cos(n\varphi+\theta_q) \qquad \textbf{(11b)}$$

The combination of modes best reproducing (or correcting) W_z will now be given by:

$$W_a(\rho,\varphi) = \sum_{n,nj} 2\alpha_{n,nj}\, Msn(\rho,\varphi,\psi_{nj}) + \alpha_0 + \alpha_d\, \rho^2 \qquad \textbf{(12a)}$$

$$Msn(\rho,\varphi,\psi_{nj}) = f_n(\rho)\, \cos(l_n(\varphi+\psi_{nj})) \qquad \textbf{(12b)}$$

where $\alpha_{n,nj}$ and ψ_{nj} specifies the strength and orientation of the modal deformation in question. The last two terms represent the (not interesting) constant phaseshift and the defocus needed to obtain the best fit. The α's and the ψ's providing the best fit of W_a to W_z can be found minimizing the sum of squared errors (again neglecting the slightly uneven ρ spacing)

$$\epsilon^2 = \sum_{all\ points} \rho\, [W_z(\rho,\varphi) - W_a(\rho,\varphi)]^2 \qquad \textbf{(13)}$$

As a result of the angular orthogonality of the functions involved this results in:

1) A given aberration term can only be reproduced by modes having the same type of angular dependance:
   $l_n = n$

2) The phase ψ_{nj} of the used modes must satisfy:
   $\theta_q = n\psi_{nj}$
   i.e. the modes must have the same orientation as the aberration to be reproduced.

These results confirm the classification of the modes in the four groups associated with the individual aberrations as stated in the end of the previous section. They also outline the strategy for creating an aberration Z_q with a given strength a_q and orientation θ_q:

1) Rotate the force patterns for the relevant modes to the orientation (if any) specified by θ_q.

2) Determine the characteristic combination L_q of modes reproducing Z_q as good as possible

$$Z_q(\rho,\varphi) \propto L_q(\rho,\varphi) = \sum_n 2\beta_n \, Msn(\rho,\varphi) \tag{14a}$$

$$Z_q(\rho,\varphi) \propto L_q(\rho,\varphi) = \sum_n 2\beta_n \, Msn(\rho,\varphi) + \beta_0 + \beta_d \, \rho^2 \quad (\textit{Rotational symmetry}) \tag{14b}$$

from the equations:

$$\begin{Bmatrix} b_{11} & . & . & b_{1m} \\ . & . & . & . \\ . & . & . & . \\ . & . & . & . \\ b_{m1} & . & . & b_{mm} \end{Bmatrix} x \begin{Bmatrix} 2\beta_1 \\ . \\ . \\ . \\ 2\beta_m \end{Bmatrix} = \begin{Bmatrix} c_1 \\ . \\ . \\ . \\ c_m \end{Bmatrix} \tag{15a}$$

(include β_0, β_d, c_0, and c_d for the case of rotational symmetry)

where

$$b_{ij} = \sum_{all\ points} \rho \; Msi(\rho,\varphi) \; Msj(\rho,\varphi) \tag{15b}$$

$$c_i = \sum_{all\ points} \rho \; Msi(\rho,\varphi) \; Z_q(\rho,\varphi) \tag{15c}$$

(include terms with Ms0 = 1 and Msd = ρ^2 for the case of rotational symmetry)

The factor 2 associated with the modal combinations reflects the fact that a given change of shape induces the double change in the optical path.

Note that if the modal shapes could be perfectly excited by the point forces (which was not the case), all elements b involving two different modal shapes would be zero.

3) Multiply the characteristic combination with a_q to obtain the correct strength.

The relative goodness of the fit to a given aberration term can be estimated from

$$\sigma^2_{Rel} = \frac{\sum_{all\ points} \rho\ [Z_q - L_q]^2}{\sum_{all\ points} \rho\ Z_q^2} \qquad \textbf{(16a)}$$

$$\sigma^2_{Rel} = \frac{\sum_{all\ points} \rho\ [Z_q - L_q]^2}{\sum_{all\ points} \rho\ [Z_q - L_0]^2} \qquad \textit{(Rotational symmetry)} \qquad \textbf{(16b)}$$

where L_0 represents the fit obtained using only a constant and defocus in the case of rotational symmetry. σ^2_{Rel} represents the relative reduction of the wavefront variance associated with a specific aberration term which can be obtained by the used modal combination.
When the characteristic force patterns associated with the individual aberration terms have been determined, a linear combination of the aberrations can be corrected by subjecting M1 to the same linear combination of these force patterns each rotated correctly.
From fitting the modal shapes (not normalized) to the individual aberration terms using the procedure outlined above, the following results were obtained:

Spherical aberration

A spherical aberration coefficient

$a_4 \quad = 10^{-3}$ mm

can be obtained using the characteristic combination

$L_4 \quad = 2\beta_2\, Ms2 + 2\beta_7\, Ms7 + \beta_0 + \beta_a\, \rho^2$

where

β_0 = -2.429 x 10^{-3} mm
β_d = 3.573 x 10^{-3} mm $\Rightarrow \delta_1$ = 111 x 10^{-3} mm (from Eq. (6c))
$2\beta_2$ = -2.256 (Dimensionless)
$2\beta_7$ = -4.107 (Dimensionless)

Minimizing the fitting error only by means of defocussing and adding a constant results in

$$L_0 = \beta_0 + \beta_d \rho^2$$

where

β_0 = -1.853 x 10^{-4} mm
β_d = 1.051 x 10^{-3} mm

The relative variance reduction obtained using Eq. (16b) is given by

σ^2_{Rel} = 8.85 x 10^{-3}

Fig. 8 shows a plot of Z_4 - L_4 and Z_4 - L_0 (for 10^{-3} mm amplitude of Z_4) as a function of the radius vector in M1 visualizing the aberration reduction which can be obtained using Ms2 and Ms7 (see Figs. 3 and 7) for correction of spherical aberration.

Astigmatism

An astigmatic coefficient

a_5 = 10^{-3} mm

can be obtained by the characteristic combination

$$L_5 = 2\beta_1 \, Ms1 + 2\beta_6 \, Ms6$$

where

$2\beta_1$ = 7.057 x 10^{-1} (Dimensionless)
$2\beta_6$ = -3.715 x 10^{-1} (Dimensionless)

Use of the results from extracting tilt and translation (see Eqs. (10)) and of Eq. (9) shows that this modal correction will result in a change of pointing

α = 0.147 arcsecs

which is considered to be negligible.
The relative variance reduction obtained using Eq. (16a) is given by

$\sigma^2_{Rel} = 5.48 \times 10^{-4}$

Fig. 9 shows a plot of Z_5 (10^{-3} mm amplitude) and $Z_5 - L_5$ visualizing the aberration reduction which can be obtained using Ms1 and Ms6 (se Figs. 2 and 6) for correction of astigmatism.

Triangular coma

A triangular coma coefficient

$a_6 = 10^{-3}$ mm

can be obtained by

$L_6 = 2\beta_3$ Ms3

where

$2\beta_3 = 4.302$ (Dimensionless)

Since no tilt (and only translation) has to be extracted from the deformation pattern, use of this modal correction will result in no change of pointing.
The relative variance reduction obtained using Eqs. (16a) is given by

$\sigma^2_{Rel} = 1.93 \times 10^{-2}$

Fig. 10 shows a plot of Z_6 (10^{-3} mm amplitude) and $Z_6 - L_6$ visualizing the aberration reduction which can be obtained using Ms3 (see Fig. 4) for correction of triangular coma.

Quadratic astigmatism

A quadratic astigmatism coefficient

$a_8 = 10^{-3}$ mm

can be obtained by

$L_8 = 2\beta_5$ Ms5

where

$2\beta_5 \quad = 1.370 \times 10^{1}$ (Dimensionless)

Use of the results from extracting tilt and translation (see Eqs. (10)) and of Eq. (9) shows that this modal correction will result in a change of pointing

$\alpha \quad = 0.124$ arcsecs

which is considered to be negligible.
The relative variance reduction obtained using Eq. (16a) is given by

$\sigma^2_{Rel} \quad = 3.96 \times 10^{-3}$

Fig. 11 shows a plot of Z_8 (10^{-3} mm amplitude) and $Z_8 - L_8$ visualizing the aberration reduction which can be obtained using Ms5 (see Fig. 5) for correction of quadratic astigmatism.

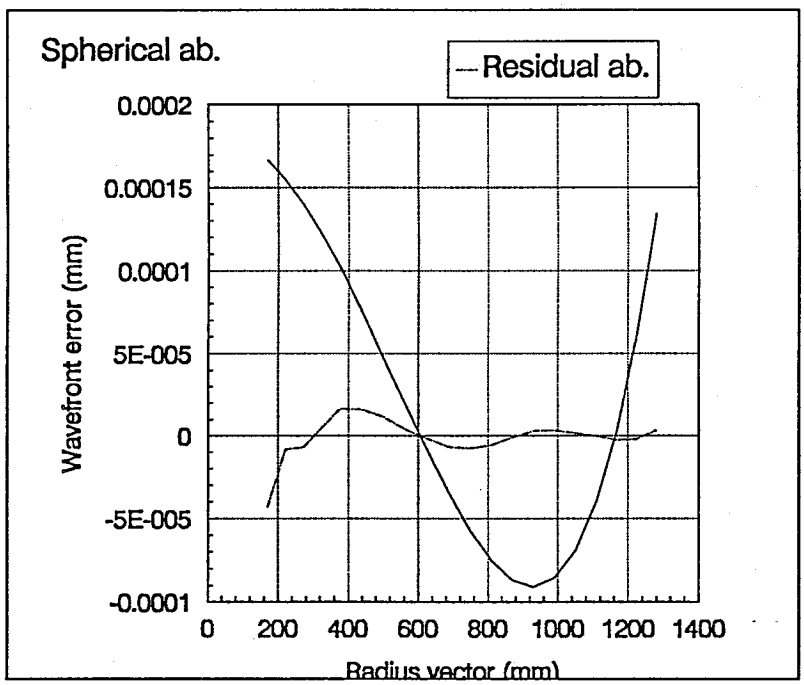

Fig. 8

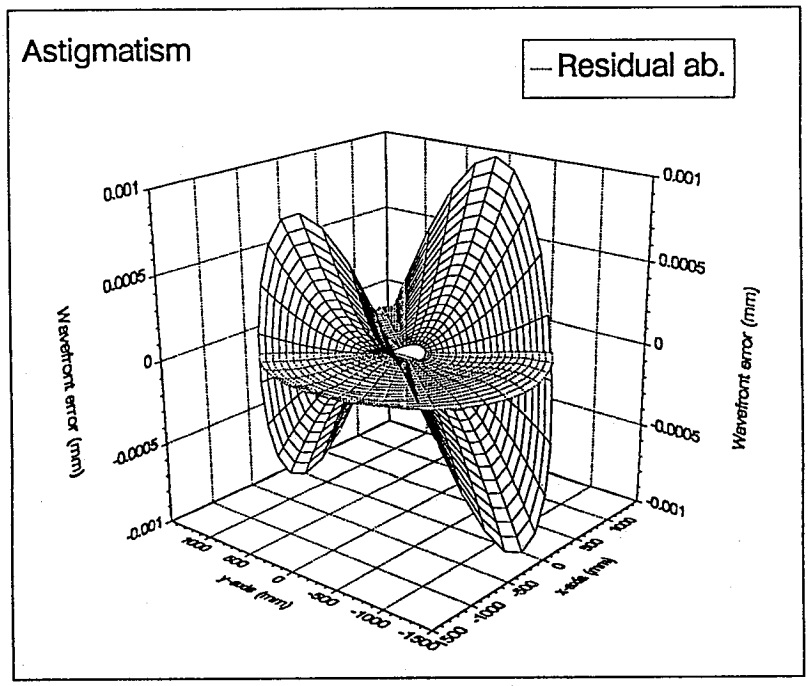
Astigmatism
Residual ab.
Wavefront error (mm)
0.001
0.0005
0
-0.0005
-0.001
y-axis (mm)
x-axis (mm)

Fig. 9

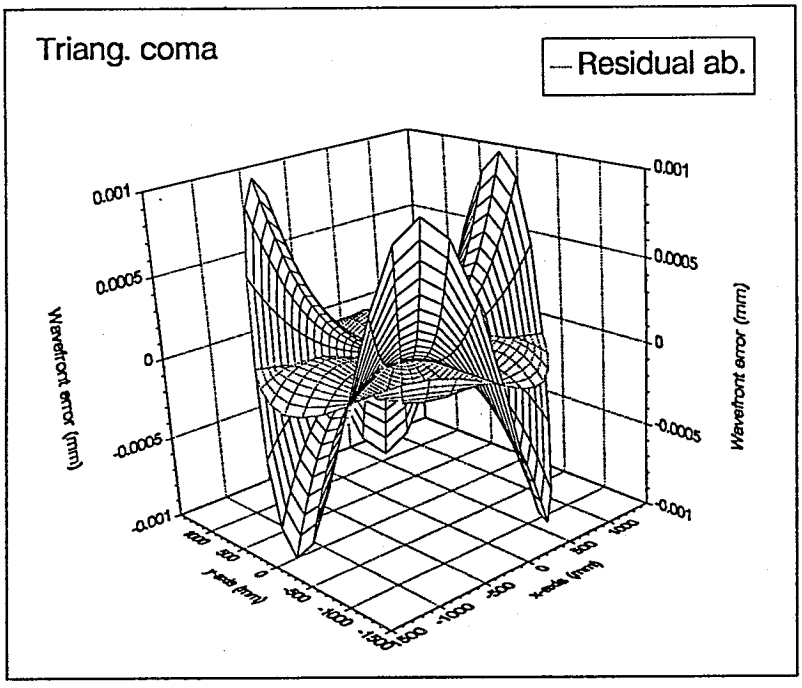
Triang. coma
Residual ab.
Wavefront error (mm)
0.001
0.0005
0
-0.0005
-0.001
y-axis (mm)
x-axis (mm)

Fig. 10

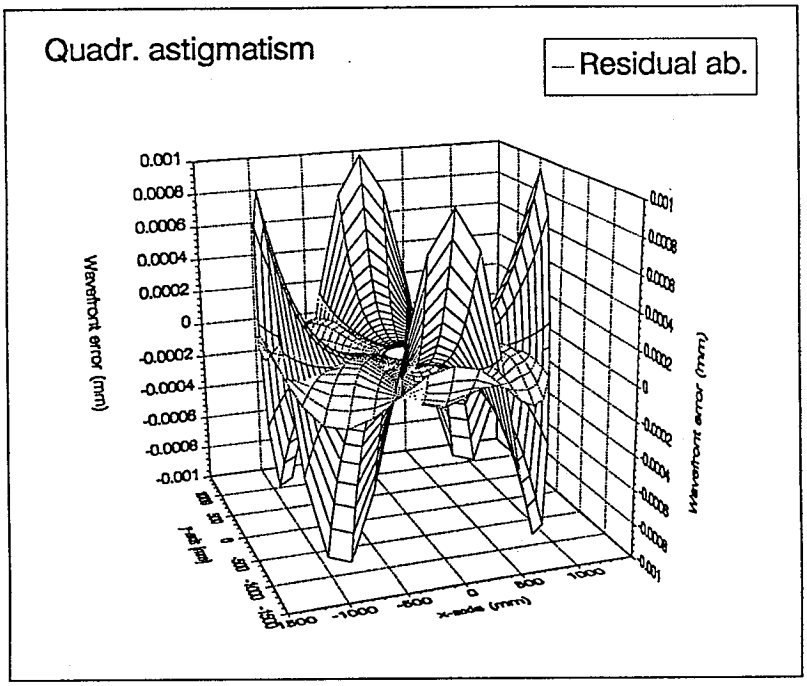
Quadr. astigmatism
Residual ab.
Wavefront error (mm)
0.001
0.0008
0.0006
0.0004
0.0002
0
-0.0002
-0.0004
-0.0006
-0.0008
-0.001
-1500
-1000
-500
0
500
1000
x-axis (mm)
Wavefront error (mm)

Fig. 11

6) Conclusion

A quantitative evaluation of the mirror control algorithms to be used for aberration reduction in NOT and the resulting expected improvements of the wavefront have been estimated. Preliminary tests with the Korhonen Hartmann wavefront sensor at NOT show that control of the aberrations treated in this report should result in a reduction of the wavefront error down to a fully satisfactory level. The approach used here is based on FE estimates of the modal shapes as also proposed in [3], followed by a calculation of the deflections arising from "modal" loading of M1 in the 45 actuator points. We believe this to be a realistic model of the actual behavior of M1 and to produce smooth deflection patterns.
It is the intention to implement the mirror control system in an open loop configuration in the beginning of 1992, and to verify that the prescribed actions result in the expected aberrations. Also the calibration of the so called "0.6 mm mechanism" for active control of decentering coma will be verified (and possibly readjusted). Later it will be investigated whether the spherical aberration showing a strong temperature dependance might also be controlled actively based on temperature measurements. The remaining aberrations will be corrected occasionally based directly on wavefront measurements.

7) References

1) Tapio Korhonen and Timo Lappalainen
Report of the Optical Tests of the Nordic Optical Telescope
Opteon April 1991

2) R. N. Wilson, F. Franza and L. Noethe
Active Optics I:
A System for Optimizing the Optical Quality and reducing the Costs of large Telescopes
ESO Scientific Reprint 484 January 1987

3) G. Gallio, R. Contro and C. Poggi
A Finite Element Approach to the Design of the Support System for the ESO 1 m Active Optics Experiment
Proceedings of the IAU Colloquium no 79, 75-93
Very large Telescopes, their Instrumentation and Programs.
Garching April 1984

4) Torben B. Andersen
Optical Specifications and Performance of the Nordic 2.5 m Telescope
NOT Scientific Association. Techn. Rep. August 1985